Journal of Hazardous Materials 173 (2010) 637–646

Contents lists available at ScienceDirect

Journal of Hazardous Materials

journal homepage: www.elsevier.com/locate/jhazmat

Adsorption of Zn^{2+} ions onto NaA and NaX zeolites: Kinetic, equilibrium and thermodynamic studies

D. Nibou [a,*], H. Mekatel [a], S. Amokrane [a], M. Barkat [b], M. Trari [c]

[a] Laboratoire des Sciences et Génie des Matériaux, Université des Sciences et de la Technologie Houari Boumediene, B.P. 32, El-Alia, Bab-Ezzouar, Alger, Algeria
[b] Centre de Recherche Nucléaire de Draria, B.P. 43, 16003 Draria, Alger, Algeria
[c] Laboratoire de stockage et de Valorisation des Energies Renouvelables, Université des Sciences et de la Technologie Houari Boumediene, B.P. 32, El-Alia, Bab-Ezzouar, Alger, Algeria

ARTICLE INFO

Article history:
Received 11 June 2009
Received in revised form 17 August 2009
Accepted 18 August 2009
Available online 1 September 2009

Keywords:
Adsorption
Zinc (II) ions
Microporous zeolite
Kinetic
Thermodynamic
Diffusion

ABSTRACT

The adsorption of Zn^{2+} onto NaA and NaX zeolites was investigated. The samples were synthesized according to a hydrothermal crystallization using aluminium isopropoxide ($Al[OCH(CH_3)_2]_3$) as a new alumina source. The effects of pH, initial concentration, solid/liquid ratio and temperature were studied in batch experiments. The Freundlich and the Langmuir models were applied and the adsorption equilibrium followed Langmuir adsorption isotherm. The uptake distribution coefficient (K_d) indicated that the Zn^{2+} removal was the highest at minimum concentration. Thermodynamic parameters were calculated. The negative values of standard enthalpy of adsorption revealed the exothermic nature of the adsorption process whereas the negative activation entropies reflected that no significant change occurs in the internal structure of the zeolites solid matrix during the sorption of Zn^{2+}. The negative values of Gibbs free energy were indicative of the spontaneity of the adsorption process. Analysis of the kinetic and rate data revealed that the pseudo second-order sorption mechanism is predominant and the intra particle diffusion was the determining step for the sorption of zinc ions. The obtained optimal parameters have been applied to wastewater from the industrial zone (Algeria) in order to remove the contained zinc effluents.

1. Introduction

Zeolites are a large group of some 70–100 different natural minerals and numerous elaborated forms [1–2]. They have a three dimensional framework consisting of silica and alumina tetrahedral units linked by shared oxygen atoms (T–O). The isomorphous replacement of Si^{4+} by Al^{3+} results in a net negative charge which is compensated by alkali and alkaline earth metal cations within the framework [3].

NaA and NaX zeolites can be prepared from a wide range of batch compositions according to Breck [3]. Also they can be made from a variety of alumina and silica source materials, e.g., pure aluminium powder or aluminium wire, fumed silica, sodium silicate, silica gels, etc. [1]. The general composition of zeolites can be represented by $M_{y/z}[(SiO_2)_x(AlO_2)_y]nH_2O$ where M is the exchangeable ion metal with a valency z. Zeolites are a suitable choice as they have a large cation exchange capacity and an affinity for heavy metals [4–9]. They are widely used as sorbents [10–14], catalysts [15–18] and cation exchangers [19–23]. The NaX zeolite cations are located in the sodalite super cage and double hexagonal rings of the zeolite framework. Super cages are able to accommodate many cations, even those with high hydrated radii, due to their aperture (8 Å) and diameter (13 Å). Sodalite and double hexagonal rings having an aperture of 2.2 Å, are less favourable to ion exchanging, because of steric factors [24]. On the other hand, the zeolite NaA cations are located in the alpha cage of the zeolite framework with an aperture of 4–5 Å, therefore favourable to ion exchanging.

Some researchers assume that diffusion of exchangeable ions through the channel/void system of zeolites is the rate determining step of the exchange process [1,3], others [21–24] believe that zeolite is an open structure whose cations are readily exchangeable with the ions present in solution. Thus, chemical exchange is slow compared to any diffusion process, i.e. the chemical exchange is the step determining mechanism [25–26]. Different mathematical models describing the diffusion process into a particle at a constant volume and pressure system were used in literature such as given by Holfferich [27] and Beyond et al. [28]. Assuming that the chemical exchange rate kinetic order is two, Blanchard et al. [29] reported that the exchange process is characterized by a linear relationship between $1/(q_\infty - q_t)$ and t; where q_∞ and q_t being the adsorption capacity at ∞ and at time t, respectively. On the other hand, the works of Turse and Rieman [30], Sinha et al. [31], and Biškup and Subotic [26] concluded that the plots $\ln(1 - q_t/q_\infty)$ vs. t should be linear if the chemical reaction is step determining.

* Corresponding author. Tel.: +213 6 63 77 97 54; fax: +213 21 24 79 19.
E-mail address: dnibou@yahoo.fr (D. Nibou).

0304-3894/$ – see front matter © 2009 Elsevier B.V. All rights reserved.
doi:10.1016/j.jhazmat.2009.08.132

Taking into consideration these approaches, we focus our attention to the use of models based on Fick's laws in the analysis of experimentally obtained data, and to determine the step describing the mechanism of the reaction according to Eq. (1) using prepared NaA and NaX zeolites with a new source of aluminium (aluminium isopropoxide ($Al[OCH(CH_3)_2]_3$)) [32].

$$Zn^{2+}{}_{(solution)} + 2Na_{(zeolite)} \leftrightarrow Zn_{(zeolite)} + 2Na^{+}{}_{(solution)} \quad (1)$$

Values of pseudo first-order and pseudo second-order rate constants were determined and interpreted. The effects of various parameters such as initial metal concentration, pH, solid–liquid ratio (R) and temperature on the exchange percentage were investigated. The obtained optimal parameters have been applied to wastewater from the industrial zone (East Algiers, Algeria) in order to remove the contained zinc effluents. The equilibrium isotherms of zinc ions sorption are also evaluated using Langmuir and Freundlich models. Thermodynamic parameters, i.e. enthalpy of adsorption $\Delta H_{ads}{}^{\circ}$, entropy change $\Delta S_{ads}{}^{\circ}$ and Gibbs free energy $\Delta G_{ads}{}^{\circ}$ for the sorption of zinc ions on NaA and NaX zeolites were examined.

2. Materials and methods

2.1. Zeolite preparation

In the present study, we used aluminium isopropoxide ($Al[OCH(CH_3)_2]_3$) as a new alumina source. NaA and NaX zeolites are prepared from gels with respectively molar compositions 1.1 Na_2O, 1 Al_2O_3, 1.26 SiO_2, 92 H_2O, and 4.8 Na_2O, 1 Al_2O_3, 3.8 SiO_2, 224 H_2O. A typical preparation for NaX was performed as follows. Distilled water (21.6 g) and a solution of sodium hydroxide (2.1 g) were added to 1.23 g of fumed silica. After stirring for 2 h, 2.2 g of aluminium isopropoxide was gradually added under continuous stirring. Finally, the whole mixture was stirred for further 2 h and kept over 24 h for incubation. The preparation of NaA zeolite was performed in the same conditions. The gels were hydrothermally reacted in Teflon-lined stainless steel autoclaves at 100 °C for 24 h. Thereafter, the products were recovered by filtration, washed with distilled water and dried at 100 °C overnight. The as-prepared forms of zeolites were calcined by heating at 600 °C during 6 h in air.

2.2. Zeolite characterization

NaA and NaX zeolites were characterized by X-ray powder diffraction (Philips PW 1800, using Cu Kα radiation), at a scan range 2θ from 5 to 50°. Surface morphology was observed by using scanning electronic microscopy (Philips XL 30) equipped with energy dispersive spectrometry for chemical analysis. The samples were coated with a thin film of carbon. Infrared spectroscopy measurements of framework vibrations were conducted using Philips PU 9800 equipment. The samples were diluted in KBr and compressed to give zeolite self-supported pellets. Thermogravimetry and differential thermal analysis (M2 BDL-Setaram) were carried out with a heating rate of 5 °C/min in the range from 25 to 900 °C. Surface area measurements were conducted using Micrometrics ASAP 2010 apparatus. Before each adsorption experiment, the calcined samples were outgassed at 350 °C overnight.

2.3. Reagents

Solutions of zinc (II) were prepared by dissolving weighed amounts of $ZnCl_2$ (Merck) in distilled water at the needed initial concentration. For zeolite preparation, the reagents used were NaOH (98%, Merck), aluminium isopropoxide ($Al[OCH(CH_3)_2]_3$) (98%, Aldrich) and fumed silica (100%, Merck) and distilled water.

2.4. Batch adsorption studies

The ion exchange of zinc (II) on NaA and NaX zeolites was carried out using the batch method. Batch adsorption experiments were conducted using different amounts of adsorbent with 100 mL of solution containing zinc metal ions. The content was agitated with a constant stirring rate at 200 rpm. The exchanged sodium Na^+ ions were monitored by ion selective potentiometric method [19] using sodium and Ag/AgCl reference electrodes and Radiometer potentiometer model. The zinc ions were determined using Eq. (1).

The adsorption percentage (Eq. (2)) was calculated by using the following equation:

$$\text{Adsorption}\,(\%) = \frac{(C_i - C_{eq})100}{C_i} \quad (2)$$

where C_i and C_{eq} are the initial and the final concentrations of the studied metal ion in its aqueous solution.

The uptake distribution coefficient K_d (Eq. (3)) is defined as the concentration of the species adsorbed per gram of the adsorbent divided by its concentration per mL in the liquid phase.

$$K_d = \frac{(C_i - C_{eq})V}{C_{eq}m}\,(\text{mL/g}) \quad (3)$$

where V is the volume of the solution in mL and m is the mass of adsorbent in grams.

3. Results and discussion

3.1. Characterization of elaborated zeolites

Fig. 1 shows XRD patterns of the prepared NaA and NaX samples. They correspond to sodalite NaA and faujasite NaX structure with strong peaks in the 2θ ranges of 5–35°, which indicates that the microporous structure of zeolites were well obtained. The two zeolites are observed as major phases and are in good agreement with those reported in the literature [32–34]. The measured XRD patterns are compared with existing ones given in the collection of simulated XRD powder patterns for zeolites [33]. All peak positions of the prepared zeolites are also indexed. The Miller indices ($h\,k\,l$) are assigned to each NaA and NaX diffraction planes as shown in Fig. 1.

Scanning electronic micrographs (Fig. 2) show that the crystallites of NaA and NaX form fine cubic particles with an average size of 4 and 3 μm respectively. Fig. 2(a) shows that NaA zeolite crystallized from amorphous gels forms cubic particles with clearly visible facets. It seems that the low sodium concentration of NaOH gels had a positive influence on the crystal morphology.

The chemical analysis gives molar Si/Al ratios of 1.2 for NaA and 3.2 for NaX which are higher than the ratios used initially as raw materials. Fig. 3 shows FT-IR spectra of elaborated NaA and NaX zeolites. The bands at 1200–450 cm^{-1} are known to be assigned to Si–O–Al, Si–O–Si, Si–O and Al–O species [3]. The band at 660 cm^{-1} is ascribed to assignable to Si–O–Me where Me is the exchangeable Na^+ ion metal species [35]. When closely examined, the absorption band at 660 cm^{-1} in NaA is large and more visible due to incorporated Na atoms in the zeolite framework (Fig. 3(a)). These bands due to vibrations of external linkages are often very sensitive to the structure. In the far infrared region (200–50 cm^{-1}), vibrations of cations as Na^+ against the framework occur [35].

TG characterization of prepared NaA and NaX in air flow show total weight losses at 900 °C of 37 and 33 wt.% respectively. DTA profiles of NaA and NaX show endothermic transformations at 150 °C which are ascribed to desorption of water located in the zeolite channels. The second transformation appears at 273 °C and is due to the decomposition of organic template used as aluminium

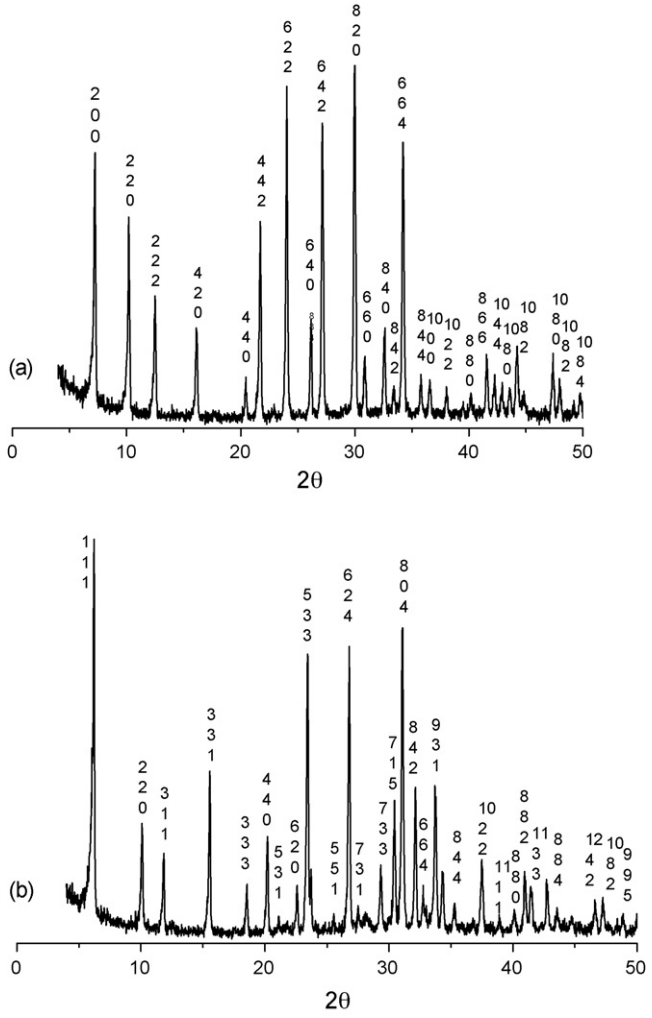

Fig. 1. XRD patterns of as-elaborated (a) NaA and (b) NaX zeolites.

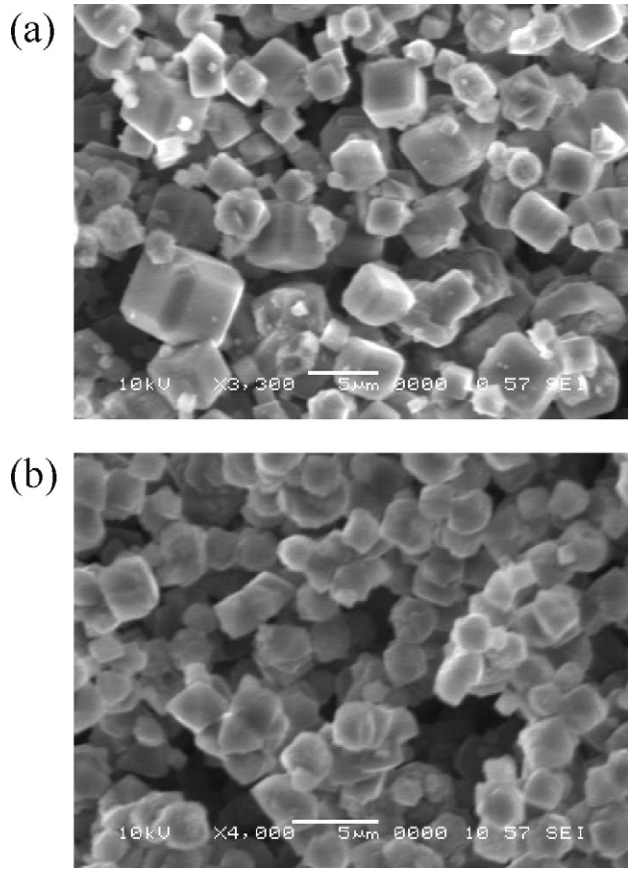

Fig. 2. Scanning electronic micrographs of elaborated (a) NaA and (b) NaX zeolites.

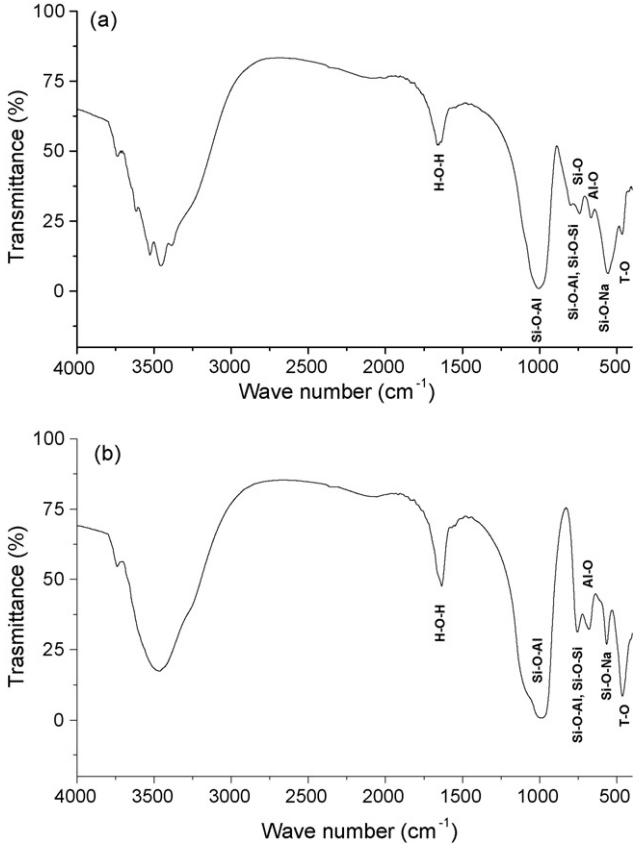

Fig. 3. FT-IR spectra of elaborated (a) NaA and (b) NaX zeolites.

reagent during the preparation of zeolites. The surface areas of prepared samples were measured by BET method [3]. The results show that high values were obtained for both NaA (280 m^2/g) and NaX (375 m^2/g).

3.2. Effect of experimental conditions on adsorption processes

3.2.1. Effect of initial concentration

The adsorption of Zn^{2+} ions onto NaA and NaX as a function of the initial zinc (II) concentrations was studied at 25 °C by varying the metal concentration from 10 to 300 mg/L. All other parameters were kept constant. The results in Fig. 4(a) showed that the uptake adsorption of zinc (II) decreases with an increase in the solution concentration indicating that fewer favourable sites become involved when solution concentration rises.

The recovery of zinc ions occurs by two well-known processes, the ion exchange and adsorption. The zinc (II) ions move through the pores and channels of NaA and NaX and are exchanged with sodium (I) ions. If the diffusion of exchangeable ions was faster in pores of zeolites and slower in smaller channels, the recovery of zinc ions proceeds via ion exchange reaction [36].

The variation of distribution factor K_d as function of initial zinc concentration is illustrated in Fig. 4(b). The K_d values decrease for both NaA and NaX with an increase of initial concentration of zinc indicating that less favourable media become involved when solution concentration increases. The maximal levels of uptake

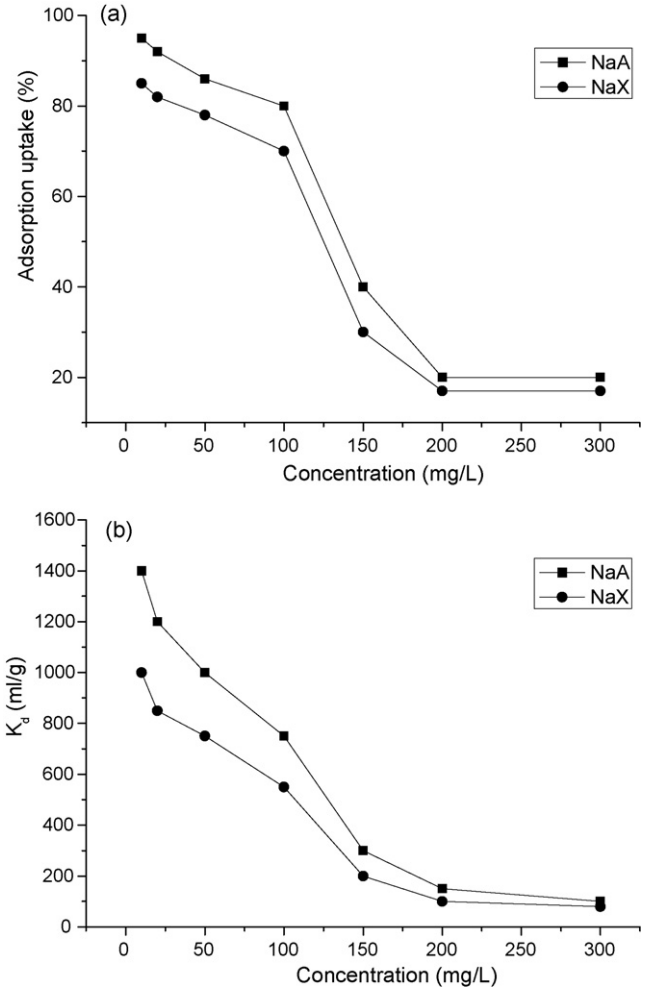

Fig. 4. Variation of adsorption uptake (a) of zinc (II) ions and K_d (b) on NaA and NaX zeolites with the initial concentration. S/L = 2.5, pH 6, T = 25 °C and t = 2 h.

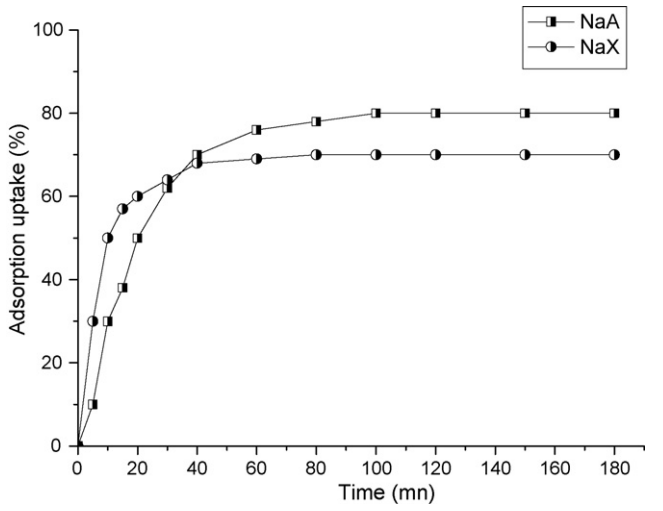

Fig. 5. Effect of contact time on the adsorption uptake of zinc (II) from aqueous solutions onto zeolites NaA and NaX. S/L = 2.5, $[Zn^{2+}]$ = 100 mg/L, pH 6 and T = 25 °C.

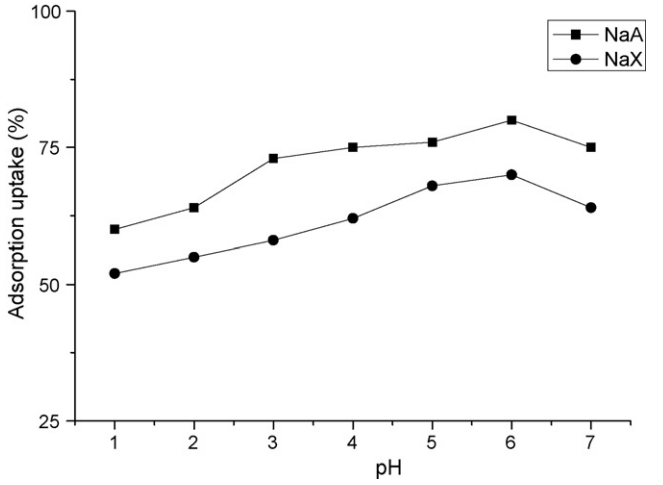

Fig. 6. Effect of pH on the adsorption uptake of zinc (II) from aqueous solutions onto zeolites NaA and NaX. S/L = 2.5, $[Zn^{2+}]$ = 100 mg/L, t = 2 h and T = 25 °C.

adsorption reached were 95 and 85% with zinc initial concentration of 10 mg/L for both zeolites NaA and NaX, respectively. However, the properties of the wastewater from the industrial zone (East Algiers, Algeria) given in Table 1 show that the zinc concentration is around 80–100 mg/L. Taking into consideration these properties, the following experimental conditions on adsorption processes were carried out at a concentration of 100 mg/L.

3.2.2. Time of equilibrium

The effect of contact time on zinc (II) adsorption was studied. The results are shown in Fig. 5, where the efficiency increases rapidly and more than 60% of the adsorbed metal occurred within 30 min using NaA and NaX zeolites. It seems that 80 and 100 min are needed to reach the equilibrium. We noticed in the present study that 120 min were taken as adequate time for equilibrium.

3.2.3. Effect of pH

In order to study the dependence of the removal efficiency on pH, experiments were conducted in the pH range 1–7 and the results are illustrated in Fig. 6. The uptake adsorption of the zinc (II) ions by the synthesized zeolites NaA and NaX increases with an increase in pH value. In the subsequent investigations, experiments were performed at solution pH value of 6 to avoid any possible hydroxide precipitation [37–39].

3.2.4. Effect of temperature

The uptake adsorption of zinc (II) ions onto both NaA and NaX zeolites at different temperatures 298, 303, 313 and 323 K are presented in Fig. 7. The results showed that the uptake adsorption decrease with the increase in temperature. This indicates an exothermic nature of the process and the adsorption of zinc (II) ions onto NaA and NaX is favoured at low temperature.

Table 1
Some physico-chemical properties of the wastewater from effluent issued from the industrial zone (East Algiers, Algeria).

pH	T (°C)	Color (mg/L, scale Pt–Co)	OD (mg/L)	BOD (mg/L)	COD (mg/L)	Organic matters (%)	Turbidity (NTU)	Zinc (II) concentration (mg/L)
5.9	25	1332	1.21	3010	24670	<1	1723	80–100

where OD, oxygen dissolved; BOD, biochemical oxygen demand; COD, chemical oxygen demand; NTU.

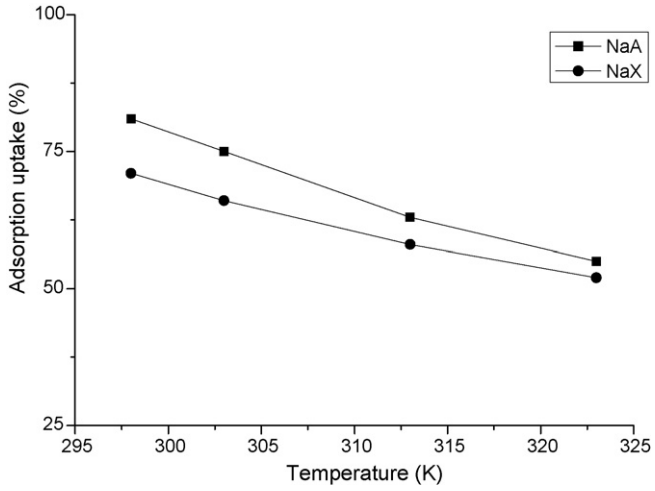

Fig. 7. Effect of temperature on the adsorption uptake of zinc (II) from aqueous solutions onto zeolites NaA and NaX. S/L = 2.5, $[Zn^{2+}]$ = 100 mg/L, t = 2 h, and pH 6.

3.3. Equilibrium isotherms

The study of equilibrium isotherms is fundamental in supplying the essential information required for the design of the sorption process. In this investigation, Langmuir and Freundlich isotherm models were used to analyse the equilibrium data by means of NaA and NaX sorbents. Langmuir Eq. (4) and Freundlich Eq. (5) isotherm models can be expressed by the following equations [40–41]:

$$q_e = \frac{Q_o b C_e}{1 + bC_e} \quad (4)$$

$$q_e = K_f C_e^{1/n} \quad (5)$$

where q_e is the equilibrium uptake (mg/g), C_e is the equilibrium zinc ions concentration (mg/L), Q_o (mg/g) (saturated monolayer sorption capacity) and b (L/g) (sorption equilibrium constant) are the Langmuir constants, K_f (L/g) and n are Freundlich constants. The linearized forms of Langmuir and Freundlich equations are given by Eqs. (6) and (7).

$$\frac{C_e}{q_e} = \frac{1}{Q_o b} + \frac{C_e}{Q_o} \quad (6)$$

$$\log q_e = \log K_f + \frac{1}{n} \log C_e \quad (7)$$

The Langmuir and Freundlich adsorption isotherms of zinc (II) on zeolites NaA and NaX are shown in Fig. 8. The model parameters and the statistical fits of the sorption data to these equations are given in Table 2. The results show that Langmuir model describes better the sorption data with a correlation factor R^2 values > 0.996. According to the saturated monolayer sorption capacity Q_o (mg/g) and b (L/g), the prepared zeolite NaA adsorbs better than zeolite NaX.

On the other hand, the equilibrium data were analysed using Freundlich isotherm model and R^2 values were estimated as 0.856 and 0.956 for NaA and NaX respectively. The value of $1/n < 1$ generally indicates that adsorption capacity is only slightly suppressed

Table 2
Langmuir and Freundlich constant values of adsorbents (T = 298 K, S/L = 2.5, $[Zn^{2+}]$ = 100 mg/L, t = 2 h, and pH 6).

	Langmuir constants				Freundlich constants		
	Q_0 (mg/g)	b (L/g)	R^2	R_L	K_f (L/g)	$1/n$	R^2
NaA	118.906	0.021	0.996	0.154	85.541	0.338	0.856
NaX	106.382	0.033	0.998	0.132	77.239	0.395	0.956

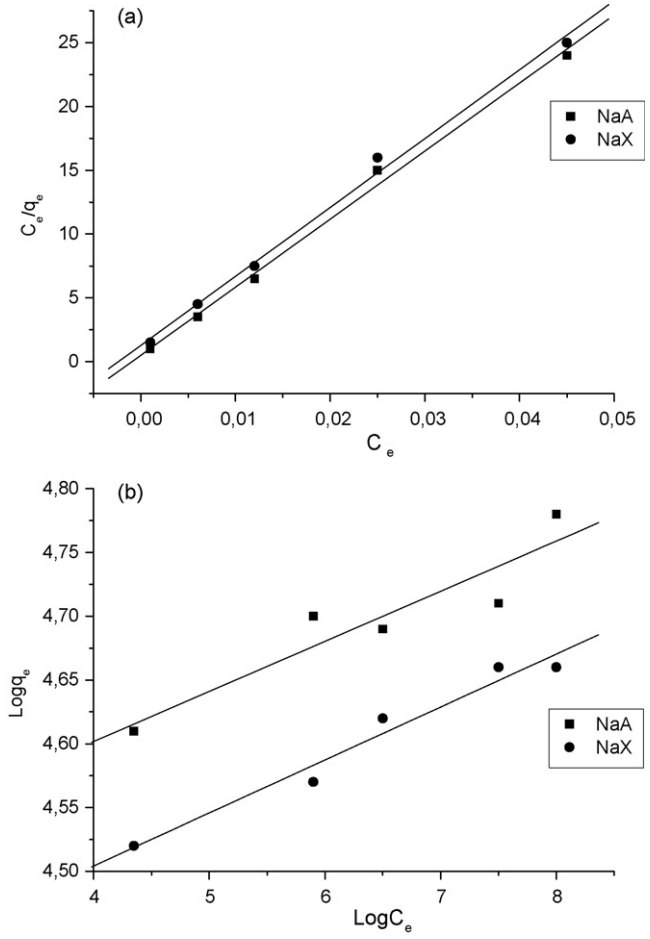

Fig. 8. Langmuir (a) and Freundlich (b) isotherms for adsorption of zinc (II) on zeolites NaA and NaX. T = 298 K, S/L = 2.5, $[Zn^{2+}]$ = 100 mg/L, t = 2 h, and pH 6.

at lower equilibrium concentrations. This isotherm does not predict any saturation of the zeolites by the zinc (II) ions; thus infinite surface coverage is expected to occur indicating multilayer adsorption on the surface [40]. It can be concluded from Table 2 that the Langmuir isotherm was more suitable than the Freundlich one as in most cases the correlation coefficient was higher as seen in Table 2. Thus, indicating the applicability of monolayer coverage of the zinc (II) on the surface of adsorbents. This can be explained by the fact that zeolites have a high surface area for metal adsorption. Therefore, only monolayer adsorption occurred on their surfaces, in spite of any surface modification. According to the literature [41], the essential characteristics of Langmuir isotherm can be explained in terms of a dimensionless constant separation factor, R_L, defined by:

$$R_L = \frac{1}{1 + bC_o} \quad (8)$$

The values of R_L indicated the type of Langmuir isotherm to be irreversible ($R_L = 0$), favourable ($0 < R_L < 1$), linear ($R_L = 1$) or unfavourable ($R_L > 1$). The calculated values of R_L shown in Table 2 indicated that adsorption of zinc (II) onto NaA and NaX zeolites was favourable in both cases.

3.4. Adsorption dynamics

The study of adsorption dynamics describes the solute uptake rate and evidently this rate controls the residence time of adsorbate uptake at the solid–solution interface. The kinetics of zinc (II) adsorption on the NaA and NaX were analysed using pseudo first-order and pseudo second-order kinetic models [42–43]. The pseudo

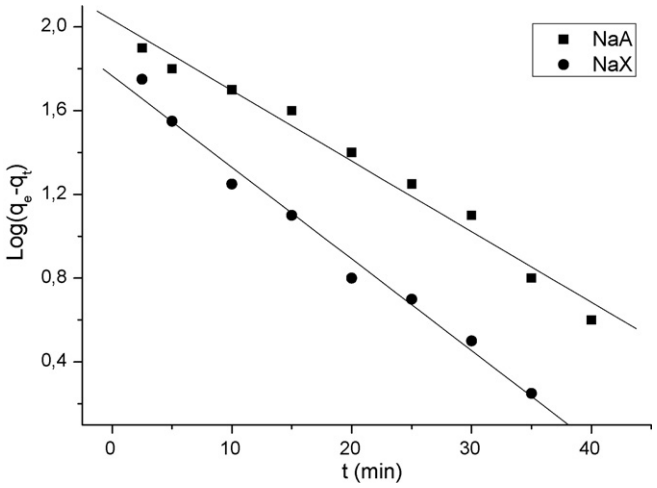

Fig. 9. Lagergren plots for the sorption of zinc (II) ions from aqueous solutions onto zeolites NaA and NaX at T = 298 K, S/L = 2.5, [Zn^{2+}] = 100 mg/L, and pH 6.

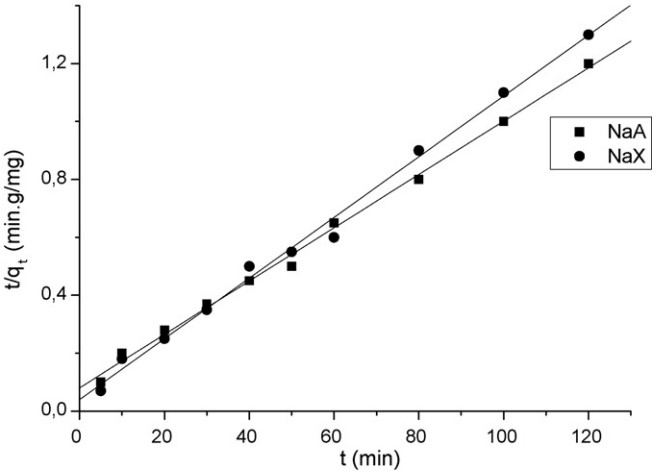

Fig. 10. Pseudo second-order kinetic plots for the sorption of zinc (II) ions from aqueous solutions onto zeolites NaA and NaX at T = 298 K, S/L = 2.5, [Zn^{2+}] = 100 mg/L, and pH 6.

first-order expressed by Lagergren equation is as follows:

$$\frac{dq_t}{dt} = k_{1ads}(q_e - q_t) \quad (9)$$

where q_e and q_t are the adsorption capacity at equilibrium and at time t, respectively (mg/g), k_{1ads} is the rate constant of pseudo first-order adsorption (min^{-1}). After integration and applying boundary conditions $t = 0$ to $t = t$ and $q_t = 0$ to $q_t = q_t$, the integrated form of Eq. (9) becomes:

$$\log(q_e - q_t) = \log q_e - \frac{k_{1ads}t}{2.303} \quad (10)$$

The values of $\log(q_e - q_t)$ were linearly correlated with t. The plot of $\log(q_e - q_t)$ vs. t should give a linear relationship from which k_{1ads} and q_e can be determined from the slope and intercept of the plot, respectively (Fig. 9).

The pseudo second-order adsorption kinetic rate equation is expressed by Eq. (11):

$$\frac{dq_t}{dt} = k_{2ads}(q_e - q_t)^2 \quad (11)$$

where k_{2ads} is the rate constant of pseudo second-order adsorption (g/mg min).

For the boundary conditions $t = 0$ to $t = t$ and $q_t = 0$ to $q_t = q_t$, the integrated form of Eq. (11) becomes:

$$\frac{1}{q_e - q_t} = \frac{1}{q_e} + k_{2ads}t \quad (12)$$

which is the integrated rate law for a pseudo second-order reaction. Eq. (12) can be rearranged to obtain Eq. (13).

$$\frac{t}{q_t} = \left(\frac{1}{k_{2ads}q_e^2}\right) + \left(\frac{t}{q_e}\right) \quad (13)$$

If the initial adsorption rate, h (mg/g min) is:

$$h = k_{2ads}q_e^2 \quad (14)$$

then Eqs. (13) and (14) become:

$$\frac{t}{q_t} = \left(\frac{1}{h}\right) + \left(\frac{t}{q_e}\right) \quad (15)$$

The plot of (t/q_t) and t of Eq. (13) should give a linear relationship from which q_e and k_{2ads} can be determined from the slope and intercept of the plot, respectively (Fig. 10). The results presented in Figs. 9 and 10 are obtained at 298 K and that those obtained in the other studied temperatures are not shown. The results of fitting experimental data with the pseudo first-order and pseudo second-order models for adsorption of zinc (II) onto NaA and NaX zeolites are presented in Table 3.

As can be seen, the correlation coefficients (R^2) are 0.99 for the pseudo second-order model and 0.94–0.97 for the pseudo first-order model, indicating a better fit with the pseudo second-order model. The better fit of this model to the experimental data is also seen in the much closer agreement between the experimental values for q_e and those from the second-order model, when compared to the q_e values generated from the first-order model. From Table 3, it can be shown that the values of initial sorption rate (h) and rate constant increased with the increase in temperature. These results

Table 3
Adsorption kinetic models rate constants for exchanged NaA and NaX at different temperatures (T = 298 K, S/L = 2.5, [Zn^{2+}] = 100 mg/L, t = 2 h, and pH 6).

T (K)	Pseudo first-order			Pseudo second-order				
	q_e(cal) (mg g^{-1})	$k_{1ads} \times 10^2$ (min^{-1})	R^2	q_e(cal) (mg g^{-1})	$k_{2ads} \times 10^3$ (g mg^{-1} min^{-1})	h (mg g^{-1} min^{-1})	R^2	q_e(exp) (mg g^{-1})
NaA								
298	108.56	7.36	0.94	117.37	0.60	8.265	0.99	118.54
303	106.32	6.58	0.95	117.69	0.62	8.587	0.99	119.76
313	110.76	8.06	0.96	118.45	0.71	10.111	0.99	121.56
323	111.90	8.53	0.97	118.57	0.72	10.122	0.99	122.21
NaX								
298	73.18	11.50	0.95	96.15	0.86	7.950	0.99	94.17
303	75.39	12.81	0.97	96.43	0.87	8.089	0.99	95.48
313	76.45	13.43	0.96	97.52	0.91	8.654	0.98	96.59
323	77.76	14.09	0.94	98.87	0.99	9.677	0.99	99.12

explain that the pseudo second-order sorption model is predominant and that the overall rate constant of each ion exchange process appears to be controlled by the chemical sorption process [26,32].

3.4.1. Rate limiting

It is known that the mechanism of ion exchange can be explained by film diffusion, particle diffusion or chemical exchange [32]. Also, at an intensive stirring of the sorptive system, the intraparticle diffusion of the solute sorbed from solution to the sorbent sites could be a rate controlling mechanism. In this study, a quantitative data and models based on the Fick's laws were applied. The initial diffusion coefficients D_i, which assume a particle diffusion mechanism to be rate-limiting, were calculated from the following equations:

$$\frac{q_t}{q_\infty} = 1 - \frac{6}{\pi^2}\sum_{n=1}^{\infty}\frac{1}{n^2}\exp\left(-\frac{D_i \cdot n^2\pi^2 \cdot t}{r_0^2}\right) \quad (16)$$

where q_t/q_∞ is the fractional attainment of equilibrium at time t of amounts of exchange; r_0 is the radius of crystallite particles assumed to be spherical and n is an integer. For short time, Eq. (16) can be rearranged to obtain Eq. (17).

$$\frac{q_t}{q_\infty} = \frac{6}{r_0}\left(\frac{D_i \cdot t}{\pi}\right)^{1/2} \quad (17)$$

The initial diffusion coefficients D_i are obtained from plots of q_t/q_∞ vs. $(\text{time})^{1/2}$ (Fig. 11). In this study, q_e value at 120 min of exchanged zeolites NaA and NaX respectively, are rearranged as q_∞ values. The gradient (p_1) of the initial linear portion of these curves is used typically up to (q_t/q_∞ = 0.4–0.6) and is expressed as follows:

$$p_1 = \frac{6}{r_0}\left(\frac{D_i}{\pi}\right)^{1/2} \quad (18)$$

Hence, the coefficients D_i becomes:

$$D_i = \frac{p_1^2\pi r_0^2}{36} \quad (19)$$

The D_i values calculated at different solid–liquid ratios, temperatures and concentrations for Zn^{2+} ions are presented in Table 4. It can be shown that D_i increases with increasing temperature and solid–liquid ratio, and decreases with increasing concentration of Zn^{2+} ions.

For longer operating times between zinc (II) ions from aqueous solutions and sodium (I) from zeolites NaA and NaX, Eq. (16) can be rearranged:

$$\ln\left(1 - \frac{q_t}{q_\infty}\right) = \ln\left(\frac{6}{\pi^2}\right) - \left(\frac{D_f}{r_0^2}\right)\cdot\pi^2 \cdot t \quad (20)$$

where D_f is the final diffusion coefficient. The determination of the gradient (p_2) from plots $\ln[(1 - q_t/q_e)]$ vs. t (min) (Fig. 12) gives the values of D_f.

$$p_2 = \frac{D_f}{r_0^2}\cdot\pi^2 \quad (21)$$

$$D_f = -\frac{p_2 \cdot r_0^2}{\pi^2} \quad (22)$$

It seems that the plots $\ln[(1 - q_t/q_e)]$ vs. t are straight lines for both studied zeolites. This phenomenon can explain the difference between film and particle diffusion controlling sorption process as reported in the literature [7–8]. The values of D_f calculated at different solid–liquid ratios, temperatures and concentrations for Zn^{2+} ions are presented in Table 5. D_f values increased with the increase of temperature and solid–liquid ratio, and decreased with increasing the concentration of Zn^{2+} ions. These results indicate that the

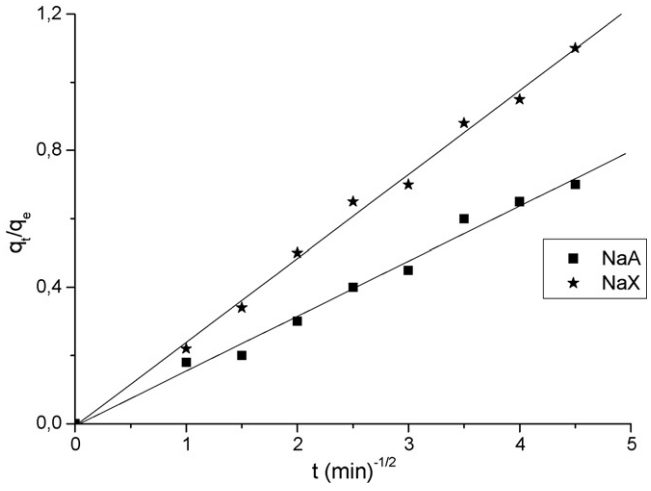

Fig. 11. q_t/q_e vs. $t^{1/2}$ plots of the early stage of the sorption of zinc (II) ions from aqueous solutions between sodium (I) from zeolites NaA and NaX with correlation coefficients R^2 equal to 0.968 and 0.969 respectively. T = 298 K, S/L = 2.5, $[Zn^{2+}]$ = 100 mg/L and pH 6.

Table 4
Coefficient diffusion D_i values of exchanged adsorbents at different solid–liquid ratios, temperatures and concentrations of zinc (II).

Solid–liquid ratio	NaA		NaX	
	$D_i \times 10^{16}$ (m^2/s)	R^2	$D_i \times 10^{16}$ (m^2/s)	R^2
2.5	12.24	0.974	8.723	0.986
2	11.13	0.987	7.813	0.982
1.5	10.37	0.999	6.563	0.991
1	9.503	0.978	5.903	0.985
0.5	8.954	0.989	5.369	0.981
at $[Zn^{2+}]$ = 100 mg/L, pH 6, T = 298 K and t = 2 h				
Temperature (K)				
298	9.550	0.986	6.525	0.999
303	10.49	0.987	7.449	0.989
313	11.59	0.987	7.999	0.981
323	12.09	0.971	8.209	0.979
at $[Zn^{2+}]$ = 100 mg/L, pH 6, S/L = 2.5 and t = 2 h				
Concentration (mg/L)				
100	12.47	0.999	8.549	0.997
150	11.11	0.963	7.763	0.976
200	9.374	0.976	6.637	0.987
250	7.033	0.998	5.991	0.998
300	6.944	0.991	5.054	0.999
at S/L = 2.5, T = 298 K, pH 6 and t = 2 h				

Table 5
Coefficient diffusion D_f values of exchanged adsorbents at different solid–liquid ratios, temperatures and concentrations of zinc (II).

Solid–liquid ratio	NaA		NaX	
	$D_f \times 10^{16}$ (m²/s)	R^2	$D_f \times 10^{16}$ (m²/s)	R^2
2.5	42.69	0.864	21.45	0.926
2	41.54	0.887	20.85	0.912
1.5	40.76	0.790	19.69	0.891
1	39.34	0.878	19.05	0.765
0.5	38.43	0.839	18.69	0.891
at $[Zn^{2+}]$ = 100 mg/L, pH 6, T = 298 K and t = 2 h				
Temperature (K)				
298	39.45	0.986	17.25	0.910
303	40.23	0.987	18.92	0.986
313	41.22	0.987	20.35	0.895
323	42.09	0.971	22.06	0.769
at $[Zn^{2+}]$ = 100 mg/L, pH 6, S/L = 2.5 and t = 2 h				
Concentration (mg/L)				
100	42.08	0.991	21.57	0.945
150	41.43	0.943	21.08	0.923
200	39.60	0.974	19.45	0.980
250	37.47	0.987	17.47	0.976
300	36.98	0.932	16.19	0.876
at S/L = 2.5, T = 298 K, pH 6 and t = 2 h				

Table 6
Thermodynamic parameters for adsorption of zinc (II) ions on NaA and NaX zeolites as function temperature (S/L = 2.5, $[Zn^{2+}]$ = 100 mg/L, t = 2 h, and pH 6).

Zeolite	ΔH° (KJ/mol)	ΔS° (J/mol K)	ΔG° (KJ/mol)			
			298[a]	303[a]	313[a]	323[a]
NaA	−30.667	−43.256	−17.777 493[b]	−17.761 735[b]	−17.128 993[b]	−16.696 1340[b]
NaX	−23.690	−22.560	−16.967 446[b]	−16.854 602[b]	−16.628 735[b]	−16.403 993[b]

[a] T (K).
[b] K_d (mL/g).

sorption process is mainly governed by particle diffusion at all the studied temperatures, concentrations and solid–liquid ratios. Coker and Rees [7] conducted detailed investigations into the kinetics of ion exchange in zeolites, and described the variation of inter-diffusion coefficients for ion exchange reactions. They have found that the diffusion of metal (II) ions into NaA zeolite is governed by two distinct diffusion coefficients, relatively fast and slower kinetics. They attributed this phenomenon to entering metal (II) ions occupying 8-ring oxygen sites which partially obstruct the pore mouths and thus increasing energy for further exchange. They calculated the initial diffusion coefficient of different metal ions such as Ca^{2+}, Sr^{2+} and Mg^{2+} adsorbed onto zeolites.

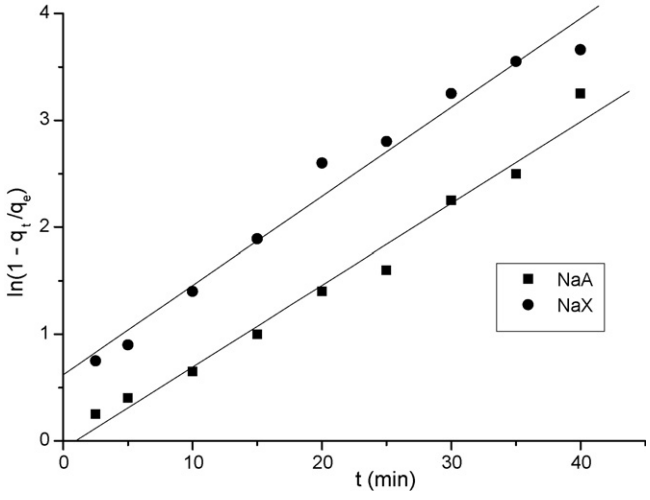

Fig. 12. $\ln[(1-q_t/q_e)]$ vs. t plots of the longer exchange times stage of the sorption of zinc (II) ions from aqueous solutions between sodium (I) from zeolites NaA and NaX with correlation coefficients R^2 equal to 0.946 and 0.953 respectively. T = 298 K, S/L = 2.5, $[Zn^{2+}]$ = 100 mg/L and pH 6.

Comparing diffusion coefficients D_i and D_f in Tables 4 and 5 shows that initial rate of exchange is almost always smaller than final rate of exchange. These results are in agreement and comparable to those reported elsewhere [7–8,44]. The activation energy E_a for the sorption of zinc (II) onto zeolites NaA and NaX was determined using the Arrhenius equation:

$$D_i = D_0 \exp^{(-E_a/RT)} \quad (23)$$

where D_0 is a pre-exponential constant.

The values of activation energy were estimated as 32.43 and 17.54 kJ/mol for NaA and NaX respectively. These results indicate that a chemical sorption process consisting of strong interaction between zeolites and Zn^{2+} and illustrate that each sorption process has a low potential energy.

The activation entropy ΔS^* for the sorption of zinc (II) onto zeolites NaA and NaX was determined using the following equation:

$$D_0 = \left(\frac{2.72d^2KT}{h}\right)\exp\left(\frac{\Delta S*}{R}\right) \quad (24)$$

where k is the Boltzmann constant, h is the Planks constant, d is the average distance between two successive positions, R is the gas constant and T is the absolute temperature. The values of ΔS^* were evaluated as −70.32 and −117.24 J/mol K for NaA and NaX respectively. These results reflect that no significant change occurs in the internal structure of the zeolites solid matrix during the sorption of zinc (II).

Table 7
Zinc (II) removal (%) by each zeolite for both solutions.

Zeolite	Solution	Zn(II)	Ref.
NaA	Synthetic solution	80.5	This work
	Industrial effluent (East Algiers)	79.6	This work
NaX	Synthetic solution	70.4	This work
	Industrial effluent (East Algiers)	68.3	This work
Natural zeolite			
Anatolia clinoptilolite	Synthetic solution	40.3	[45]
	–	–	
Mordenite	Synthetic solution	41.8	[46]
	Storm water	10.1	[46]

3.5. Thermodynamic parameters

Thermodynamic parameters as enthalpy of adsorption ΔH°, entropy change ΔS°, and free energy ΔG° for the sorption of zinc ions on NaA and NaX zeolites were calculated using the following equations:

$$\ln K_d = \left(\frac{\Delta S^\circ}{R}\right) - \left(\frac{\Delta H^\circ}{RT}\right) \quad (25)$$

$$\Delta G^\circ = \Delta H^\circ - T\Delta S^\circ \quad (26)$$

The values of ΔH° and ΔS° are obtained from the slope and the intercept of each plot ($\ln K_d$ against $1/T$ for two prepared zeolites), which were estimated by a curve-fitting program. The values of thermodynamic parameters for the sorption of zinc ions on NaA and NaX zeolites are given in Table 6. The results show that $\Delta G_{ads}{}^\circ$ becomes less negative with increasing temperature indicating that sorption is less favourable at high temperatures. In addition, the negative values of $\Delta H_{ads}{}^\circ$ indicate that the sorption of zinc (II) ions on NaA and NaX prepared zeolites is exothermic process. The exchange of zinc (II) ions as a result of adsorption is ascribed to a decrease in the degree of freedom of adsorbate ion which results in the entropy change.

3.6. Treatment of zinc (II) wastewater

Zinc (II) wastewater samples have been taken from effluent issued from the industrial zone (East Algiers). After decantation and filtration, in order to remove the dissolved pollutants (e.g. organic matter) and clarify the solution, some physico-chemical properties were obtained and presented in Table 1. Then, adsorption zinc (II) tests have been carried out onto synthetic NaA and NaX zeolites using optimal conditions previously determined. It has been found that the zinc (II) removal yield was 79.6% for NaA and 68.3% for NaX. The synthetic zeolites were found to be very effective in removing zinc (II) from both solutions.

Comparing the removal efficiencies (%) for zeolites, Table 7 shows that the synthetic zeolite performs considerably better than the natural one. The explanation is that the NaA and NaX adsorbents were pure zeolites and natural ones contain other mineral impurities such as Ca, Mg, Fe and K [45] which could interfere in the exchange of zinc with sodium ions. Moreover, NaA and NaX have small particles with an average size of 4 and 3 μm respectively and higher internal surface areas of 280 and 375 m^2/g. These characteristics allow the zinc ions to access and diffuse in the framework structures [1–3].

In addition, the organic matter content of the industrial effluent is lower (<1%) compared to storm water solution [46] and this could partly explain the higher uptake. The co-adsorption of the organic matter causes a decrease of the active sites of natural zeolite and complexes with other metals present in the structure [45].

4. Conclusion

In the present work, we report on the preparation and characterization of two sorbent zeolites NaA and NaX and their use in the adsorption of zinc (II) ions from aqueous solutions. In these syntheses, aluminium isopropoxide used as new source gave positive results. The diffusion coefficient K_d decreases both for NaA and NaX with increasing the concentration of zinc (II) ions indicating that less favourable media become involved when solution concentration increases. The values of the thermodynamic parameters show that $\Delta G_{ads}{}^\circ$ become less negative with increasing temperature indicating that sorption is less favourable at high temperatures. The negative values of $\Delta H_{ads}{}^\circ$ and ΔS^* indicate that the sorption of zinc (II) ions on prepared zeolites is exothermic process and the sorbate zinc ions are stable on the solid surface. The exchange of zinc (II) ions as a result of adsorption is ascribed to a decrease in the degree of freedom of adsorbate ion which results in the entropy change. Analysis of the kinetic and rate data revealed that the pseudo second-order sorption mechanism is predominant and the intraparticle diffusion was the determining step for the sorption of zinc ions. The optimized parameters have been applied to the wastewater from the industrial zone in order to remove the contained zinc effluents. It has been found that the zinc (II) removal yield was 79.6% for NaA and 68.3% for NaX. The synthetic zeolites were found to be very effective in removing zinc (II) from both solutions.

References

[1] R.M. Barrer, Zeolites and Clay Minerals as Sorbents and Molecular Sieves, Academic Press, London, 1978.
[2] A. Dyer, An Introduction to Zeolite Molecular Sieve, John Wiley, London, 1988.
[3] D.W. Breck, Zeolite Molecular Sieves—Structure Chemistry and Use, Wiley Interscience, New York, 1974.
[4] S. Akyıl, A. Mahmoud, A. Aslani, Distribution of uranium on zeolite X and investigation of thermodynamic parameters for this system, J. Alloys Compd. 271/273 (1998) 769–773.
[5] R. Petrus, J. Warchoł, Ion exchange equilibria between clinoptilolite and aqueous solutions of Na^+/Cu^{2+}, Na^+/Cd^{2+} and Na^+/Pb^{2+}, Microporous Mesoporous Mater. 61 (2003) 137–146.
[6] A. Benhammo, A. Yaacoubi, L. Nibou, B. Taouti, Adsorption of metal ions onto Moroccan stevensite: kinetic and isotherm studies, J. Colloid Interface Sci. 22 (2005) 320–326.
[7] E.N. Coker, L.V.C. Rees, Kinetics of ion exchange in quasi-crystalline aluminosilicate zeolite precursors, Microporous Mesoporous Mater. 84 (2005) 171–178.
[8] K.M. Abd El-Rahman, M.R. El-Sourougy, Modeling the sorption kinetics of cesium and strontium ions on zeolite A, J. Nucl. Radio. Sci. 7 (2) (2006) 21–27.
[9] A.M. El-Kamash, Evaluation of zeolite A for the sorptive removal of Cs^+ and Sr^{2+} ions from aqueous solutions using batch and fixed bed column operations, J. Hazard. Mater. 151 (2–3) (2008) 432–445.
[10] Y.S. Ho, J.F. Porter, G. McKay, Equilibrium isotherm studies for the sorption of divalent metal ions onto peat: Cu, Ni, and Pb single component systems, Water Air Soil Pollut. 141 (2002) 1–33.
[11] N. Bekta, S. Kara, Removal of lead from aqueous solutions by natural clinoptilolite: equilibrium and kinetic studies, Sep. Purif. Technol. 39 (2004) 189–200.
[12] A. Kaya, A.H. Oren, Factors affecting adsorption characteristics of Zn^{2+} on two natural zeolites, J. Hazard. Mater. B131 (2006) 59–65.
[13] K. Saltali, A. Sari, Removal of ammonium ion from aqueous solution by natural Turkish (Yildizeli) zeolite for environmental quality, J. Hazard. Mater. 141 (2007) 258–263.
[14] M. Al-Anbar, Z.A. Al-Anbar, Utilisation of zeolite as ion exchange and sorbent material in the removal of iron, Desalination 225 (2008) 70–81.
[15] G.C. Bond, Heterogeneous Catalysis—Principles and Applications, 2nd ed., Clarndou, Oxford, 1987.
[16] A. Azzouz, D. Nibou, Hydrocarbons conversions over Y-Zeolite used in uranium ore wastes treatment. Activity and selectivity of Y-faujasite modified by uranyl ions in the catalytic disproportionation of toluene, Appl. Catal. (Gen. A) 79 (1) (1991) 19–28.
[17] E. Dumitriu, N. Bilba, M. Lupascu, A. Azzouz, V. Hulea, G. Cirje et, D. Nibou, Vapor phase condensation of formaldehyde and acetaldehyde into acrolein over zeolites, J. Catal. 147 (1994) 133–139.
[18] D. Nibou, S. Amokrane, Dependence between the activity and selectivity of NaLaY and NaCeY catalysts in the catalytic disproportionation of toluene, Stud. Surf. Sci. Catal. Ser. 158 B (2005) 1645–1652.
[19] J. Vesly, D. Weiss, K. Stulik, Analysis with Ion Selective Electrodes, Wiley Interscience, New York, 1978.

[20] S. Amokrane, R. Rebiai, S. Lebaili, D. Nibou, G. Marcon, Stability study of aluminisilicate materials after iron exchange. Influence of Si/Al ratio on crystallinity, Ann. Chim. Sci. Mater. 25 (Supp. 1) (2000) S267–S270.
[21] M. Kuronen, R. Harjula, J. Jernstrom, M. Vestenius, J. Lehto, Effect of the framework charge density on zeolite ion exchange selectivities, Phys. Chem. 2 (2000) 2655–2659.
[22] M. Kuronen, M. Weller, R. Townsend, R. Harjula, Ion exchange selectivity and structural changesin highly aluminous zeolithes, React. Funct. Polym. 66 (2006) 1350–1361.
[23] D. Karadag, Y. Koc, M. Turan, A comparative study of linear and non-linear regression analysis for ammonium exchange by clinoptilolite zeolite, J. Hazard. Mater. 144 (2007) 432–437.
[24] J.C. Jansen, in: H. Van Bekkum, E.M. Flanigen, P.A. Jacobs, J.C. Jansen (Eds.), Introduction to Zeolite Science and Practice, 2nd ed., Elsevier, Amsterdam, 2001.
[25] B. Biškup, B. Subotic, Kinetcs of continious exchange of Zn^{2+}ions from solutions with Na^{+} ions from thin layer of zeolite A, Stud. Surf. Sci. Catal. 125 (1999) 745–752.
[26] B. Biškup, B. Subotic, Kinetic analysis of the exchange processes between sodium ions from zeolite A and cadmium, copper and nickel ions from solutions, Sep. Purif. Technol. 37 (2004) 17–31.
[27] F. Holfferich, Ion Exchange, McGraw Hill, New York, 1962.
[28] G.E. Beyond, A.W. Adamson, L.S. Myers, The exchange adsorption of ions from aqueous solutions by organic zeolites, J. Am. Chem. Soc. 69 (1947) 2836–2848.
[29] G. Blanchard, M. Maunaye, G. Martin, Removal of heavy metals from waters by means of natural zeolites, Water Res. 18 (1984) 1501–1507.
[30] R. Turse, W. Rieman, Kinetics of ion exchange in a chelating resin, J. Phys. Chem. 65 (1961) 1821–1824.
[31] P.K. Sinha, P.K. Panicker, R.V. Amalraj, Treatment of radioactive liquid waste containing cesium by indigeneously available synthetic zeolites: a comparative study, Waste Manage. 15 (1995) 149–157.
[32] S. Khemaissia, Ph.D. thesis, University of Science and Technology (USTHB), Algiers, 2008.
[33] M.M.J. Traecy, J.B. Higging, Collection of Simulated X Patterns for Zeolites, 4th revised ed., Elsevier, Amsterdam, 2001.
[34] H. Mekatel, Master thesis, University of Science and Technology Houari Boumediene, Algiers, Algeria, 2008.
[35] D. Nibou, Ph.D. thesis, University of Science and Technology (USTHB), Algiers, 1999.
[36] M. Targo, J. Peric, A comparative study of ion exchange kinetics in zinc/lead-modified Zeolite-clinoptilotile systems, J. Hazard. Mater. B 136 (2006) 938–945.
[37] C.P. Huang, E.A. Rhoads, Adsorption of Zn (II) onto hydrous aluminisilicates, J. Colloid Interface Sci. 131 (2) (1989) 289–306.
[38] S. Kocaoba, Y. Orhan, T. Akyüz, Kinetics and equilibrium studies of heavy metal ions removal by use of natural zeolite, Desalination 2014 (2007) 1–10.
[39] A. García-Mendieta, M. Solache-Ríosand, M.T. Olguín, Evaluation of the sorption properties of a Mexican clinoptilolite-rich tuff for iron, manganese and iron–manganese systems, Microporous Mesoporous Mater. 118 (1–3) (2009) 489–495.
[40] H. Freundlich, Adsoption in solution, Phys. Chem. 57 (1906) 384–401.
[41] L. Langmuir, Adsoption of gases on plane surfaces of glass, mica and platinum, J. Am. Chem. Soc. 40 (1918) 1361–1403.
[42] S. Lagergren, Zur theorie der sogenannten adsorption geloster stoffe Kungliga Svenska Vetenskapsakademiens, vol. 24, Handlingar, 1898, pp.1–39.
[43] D.M. Ruthven, Principles of Adsorption and Adsorption Process, John Wiley, New York, 1984.
[44] P. Yang, J. Stolz, T. Armbruster, M.E. Gunter, Na, K, Rb and Cs exchange in heulandite single cystals: diffusion kinetics, Am. Mineral. 82 (1997) 517–525.
[45] S.K. Pitcher, R.C.T. Slade, N.I. Ward, Heavy metal removal from motorway stormwater using zeolites, Sci. Total Environ. 334–334 (2004) 161–166.
[46] E. Erdem, N. Karapinar, R. Donat, The removal of heavy metal cations by natural zeolites, J. Interface Sci. 280 (2004) 309–314.